

Pressure-Induced Disordered Substitution Alloy in Sb_2Te_3 Jinggeng Zhao,^{†,‡} Haozhe Liu,^{*,†} Lars Ehm,^{‡,§} Zhiqiang Chen,[§] Stanislav Sinogeikin,^{||} Yusheng Zhao,^{⊥,#} and Genda Gu[¶][†]Natural Science Research Center, Academy of Fundamental and Interdisciplinary Sciences, Harbin Institute of Technology, Harbin 150080, China[‡]Photon Sciences Directorate, Brookhaven National Laboratory, Upton, New York 11973, United States[§]Mineral Physics Institute, Department of Geosciences, Stony Brook University, Stony Brook, New York 11794, United States^{||}High Pressure Collaborative Access Team (HPCAT), Geophysical Laboratory, Carnegie Institution of Washington, Argonne, Illinois 60439, United States[⊥]Los Alamos Neutron Science Center (LANSCE), Los Alamos National Laboratory, Los Alamos, New Mexico 87545, United States[#]High Pressure Science and Engineering Center, University of Nevada, Las Vegas, Nevada 89154, United States[¶]Condensed Matter Physics and Materials Science Department, Brookhaven National Laboratory, Upton, New York 11973, United States

Supporting Information

ABSTRACT: A new type of disordered substitution alloy of Sb and Te at above 15.1 GPa was discovered by performing in situ high-pressure angle-dispersive X-ray diffraction experiments on antimony telluride (Sb_2Te_3), a topological insulator and thermoelectric material, at room temperature. In this disordered substitution alloy, Sb_2Te_3 crystallizes into a monoclinic structure with the space group $C2/m$, which is different from the corresponding high-pressure phase of the similar isostructural compound Bi_2Te_3 . Above 19.8 GPa, Sb_2Te_3 adopts a body-centered-cubic structure with the disordered atomic array in the crystal lattice. The in situ high-pressure experiments down to about 13 K show that Sb_2Te_3 undergoes the same phase-transition sequence with increasing pressure at low temperature, with almost the same phase-transition pressures.

Recently, topological insulators have become a hot topic in the material research field. The A_2B_3 -type compounds Bi_2Te_3 , Sb_2Te_3 , and Bi_2Se_3 , composed from group V and VI elements, are the simplest three-dimensional topological insulators.¹ Bi_2Te_3 and Sb_2Te_3 also exhibit excellent thermoelectric properties.² At ambient pressure, these compounds crystallize in space group $R\bar{3}m$,³ which is denoted as phase I. The high-pressure behavior of Bi_2Te_3 has been investigated,⁴ and a sequence of three structural phase transitions has been reported in the pressure range of 0–52.1 GPa. Bi_2Te_3 transforms from its ambient rhombohedral structure to a monoclinic structure (phase II, space group $C2/m$) at about 8.2 GPa and further to a second monoclinic structure (phase III, space group $C2/c$) at about 13.4 GPa.^{4a} At pressures larger than 14.4 GPa, Bi_2Te_3 transforms to a body-centered-cubic (bcc) structure (phase IV) with a disordered array of Bi and Te atoms.⁴ Interestingly, pressure can tune Bi_2Te_3 to a topological superconductor with a highest T_c of 9.5 K at about 13.6 GPa.⁵ Therefore, pressure plays a very important role in the

researches of topological materials, which will significantly improve our understanding for the fundamental relationship between the structure and property, as well as the mechanism of superconductivity.

On the basis of the similarity of the crystal structure and chemical composition with Bi_2Te_3 , Sb_2Te_3 is expected to undergo similar structure and physical property transformation under high pressure. Previous high-pressure investigations of the crystal structure and electrical properties of Sb_2Te_3 were performed.⁶ Sb_2Te_3 transforms to a high-pressure phase at about 9 GPa at room temperature.^{6a,b} However, crystalline structures of the high-pressure phases for Sb_2Te_3 have not been solved over last 3 decades. For A_2B_3 -type topological insulators, the systematic structural evolution information under pressure is lacking as well. In this Communication, we present the discovery of pressure-induced structural transitions in Sb_2Te_3 by using a diamond anvil cell (DAC) technique combined with the in situ angle-dispersive synchrotron X-ray diffraction (ADXRD) experimental technique and discovered a new type of disordered substitution alloy of Sb and Te atoms with a monoclinic structure at above 15.1 GPa, which is a high-pressure phase different from the corresponding phase in Bi_2Te_3 .

Figure 1 shows the selected XRD patterns of Sb_2Te_3 up to 38.6 GPa at room temperature with a wavelength of 0.04067 nm. Three structural phase transitions were found in the experimental pressure range. Sb_2Te_3 recovers to the original rhombohedral structure at pressure release. At about 9.3 GPa, Sb_2Te_3 starts the transformation from the original rhombohedral structure (phase I) to a monoclinic structure (phase II) with space group $C2/m$. The transition to phase II is completed at 12.3 GPa. At pressure greater than about 15.1 GPa, the array of Sb and Te atoms in Sb_2Te_3 becomes disordered, which induces the emergence of another monoclinic structure (phase III, space group $C2/m$). This phase is a new type of disordered

Received: August 10, 2011

Published: October 18, 2011

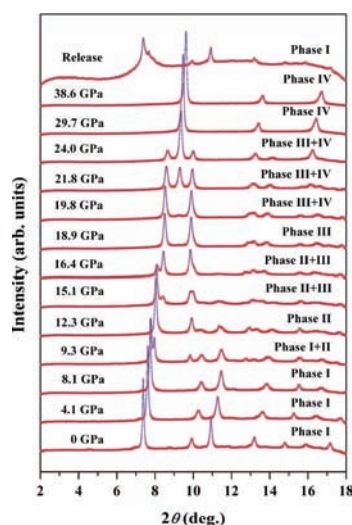


Figure 1. AD-XRD patterns of Sb_2Te_3 at room temperature up to 38.6 GPa ($\lambda = 0.04067$ nm).

substitution alloy of Sb and Te atoms and is stable only at high-pressure conditions. At about 18.9 GPa, Sb_2Te_3 completely transforms to phase III. After this, it remains its disorder characters and transforms to a bcc structure (phase IV, space group $Im\bar{3}m$) at about 19.8 GPa. Above 29.7 GPa, the transformation of phase III to phase IV is complete, and phase IV remains the stable phase up to the maximum pressure of 38.6 GPa in this investigation.

The typical Rietveld refinements results for the four phases were shown in Figure 2, in which the experimental (cross) and

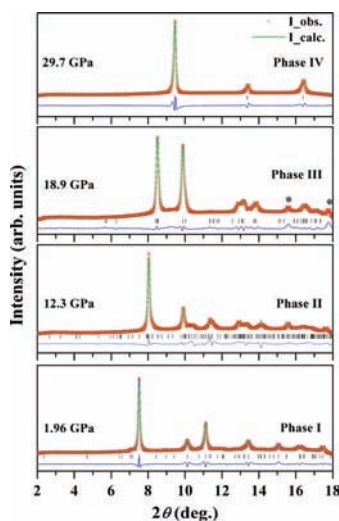


Figure 2. Experimental (cross) and fitted (line) XRD patterns for Sb_2Te_3 ($\lambda = 0.04067$ nm).

fitted (line) XRD patterns for Sb_2Te_3 were plotted for the cases of pressure at 1.96, 12.3, 18.9, and 29.7 GPa, respectively. The schematic views of the crystal structures of the four phases of Sb_2Te_3 at various pressure conditions are shown in Figure S2 of the Supporting Information. The atomic parameters of these four phases, obtained from the refinement results in Figure 2, are shown in Table S1 of the Supporting Information. The discussions about the disordered structures of phases III and IV of Sb_2Te_3 are in the annotations of Table S1 of the Supporting

Information. The main bond distances of phases I and II for Sb_2Te_3 are listed in Table S2 of the Supporting Information.

The unit cell parameters of Sb_2Te_3 at 0–38.6 GPa are derived from Le Bail refinements. The volume per Sb_2Te_3 chemical formula unit ($V/\text{Sb}_2\text{Te}_3$) is equal to $1/3$, $1/4$, $1/1.2$, and $1/0.4$ of the unit cell for phases I–IV, respectively. The relationship of $V/\text{Sb}_2\text{Te}_3$ versus pressure is shown in Figure 3.

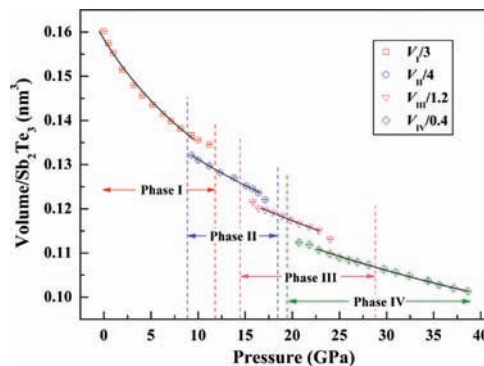


Figure 3. Pressure dependence of the volume per Sb_2Te_3 chemical formula ($V/\text{Sb}_2\text{Te}_3$). The solid lines are the fitting results according to the second-order Birch EoS.

There are four main regions in Figure 3, corresponding to the four phases of Sb_2Te_3 under high pressure. With increasing pressure, the volume is decreasing for the four phases of Sb_2Te_3 . The volume ($V/\text{Sb}_2\text{Te}_3$) collapse is about 3.3%, 2.8%, and 3.8% for the phase transitions of I–II, II–III, and III–IV, respectively. The solid lines are the fitting results for the four phases of Sb_2Te_3 using the second-order Birch equation of state (EoS).⁷ With B'_0 fixed as 4, the ambient pressure isothermal bulk modulus B_0 is estimated as 45(2), 62(3), 69(4), and 72(2) GPa for phases I–IV, respectively.

The radii of the Bi, Sb, and Te atoms are 0.160, 0.145, and 0.140 nm at ambient conditions, respectively.⁸ Both Bi_2Te_3 and Sb_2Te_3 transform to a 7-fold monoclinic structure (phase II) from the original rhombohedral structure (phase I).^{4a} The phase-transition pressure of 9.3 GPa for Sb_2Te_3 is larger than that of Bi_2Te_3 (8.2 GPa), which is due to the smaller atomic radii of the Sb to Bi atoms. The transition from phase II to III occurs at about 15.1 and 13.4 GPa for Sb_2Te_3 and Bi_2Te_3 , respectively. Although Sb_2Te_3 adopts ambient and first high-pressure forms (phases I and II) similar to those of Bi_2Te_3 , the experimental XRD patterns of phase III for Sb_2Te_3 could not be fitted using the corresponding structure model of the 8-fold monoclinic structures of Bi_2Te_3 (phase III, space group $C2/c$), as proposed in ref 4a. Sb_2Te_3 adopts a disordered monoclinic structure with space group $C2/m$ in phase III. Compared with the atomic radius of the Bi atom at ambient conditions,⁸ the atomic radius of the Sb atom is close to that of the Te atom, which indicates that disordered substitution between the Sb and Te atoms is relatively easier than that between the Bi and Te atoms. Upon compression, the potential charge transferring from Sb to Te will make the effective atomic radius of these two atoms closer. So, the disordered solution of the Sb and Te atoms begins from phase III in Sb_2Te_3 , which is different from that in Bi_2Te_3 . Under further compression, both Bi_2Te_3 and Sb_2Te_3 eventually adopt the disordered bcc structure, with phase-transition pressures of 14.4 and 19.8 GPa, respectively.⁴ Although it is easier for the Sb and Te atoms to form a disordered array, the phase-transition pressure of Sb_2Te_3 is

larger than that of Bi_2Te_3 because of the emergence of the disordered monoclinic structure of Sb_2Te_3 (phase III) from about 15.1 GPa.

The pressure-induced bcc structure is a common phase in Sb, Te, and Bi elementary substances, with phase-transition pressures of 28, 27, and 7.7 GPa, respectively.^{9,10} For binary compounds, Bi_2Te_3 reaches a bcc structure at 14.4 GPa, which is in the middle of these phase-transition pressures for the bcc structures of Bi and Te.^{4a,10a,b} However, the phase-transition pressure for the bcc structure in Sb_2Te_3 in this report is 19.8 GPa, which is smaller than the transitions in the individual elements of Sb and Te.^{9,10a,b} This lower phase-transition pressure for the bcc structure in Sb_2Te_3 could be partially caused by the disordered atom array beginning from its high-pressure phase III, and this disordered phase III makes the transition to phase IV of the bcc structure relatively easier because of the common disordered character.

The effect of low temperature on the structural evolution for A_2B_3 -type topological insulators is critical for the high-pressure property study. Therefore, in situ high-pressure XRD experiments for Sb_2Te_3 were performed at about 13 K. At low temperature, three pressure-induced first-order phase transitions were observed, which follow the same sequence as those at room temperature. These phase-transition pressures were observed to delay by about 2 GPa compared to the case at room temperature. This phase diagram in the pressure–temperature domain indicates that we could indeed explain the pressure-induced physical property change at low temperature by referring to the structural evolution with pressure at room temperature for these types of topological insulators.

In summary, three crystal structural phase transitions in topological insulator Sb_2Te_3 under high pressure within 38.6 GPa were discovered in this Communication. Because of the similar crystal structural evolution behavior under high pressure between Sb_2Te_3 and Bi_2Te_3 , a similar pressure-induced topological superconducting transition on Sb_2Te_3 can be naturally expected. Thus, the structural evolution information under pressure in Sb_2Te_3 will provide the essential guideline for the next pressure-tuned physical property evolution study. A new disordered substitution alloy of the Sb and Te atoms was found at above 15.1 GPa. The formation of atomic disordered substitution under high pressure will provide a method to obtain different types of alloys between these two elements. These pressure-induced structural transition behavior studies will improve our understanding for the universal structural evolution pattern for this A_2B_3 type of topological insulator material upon compression.

■ ASSOCIATED CONTENT

● Supporting Information

Experimental details, ruby fluorescence R1 and R2 peaks at 26.9 and 35.6 GPa (Figure S1), schematic views of the crystal structures (Figure S2), atomic parameters of phases I–IV for Sb_2Te_3 (Table S1), and the main bond distances of phases I and II for Sb_2Te_3 (Table S2). This material is available free of charge via the Internet at <http://pubs.acs.org>.

■ AUTHOR INFORMATION

Corresponding Author

*E-mail: haozhe@hit.edu.cn.

■ ACKNOWLEDGMENTS

This work was partly supported by the National Natural Science Foundation of China (Grants 10904022 and 10975042), the China Postdoctoral Science Foundation special funded project (Grant 200902410), and the program for Basic Research Excellent Talents and Oversea Collaborative Base Project in Harbin Institute of Technology (HIT). We are thankful for support from COMPRES (the Consortium for Materials Properties Research in Earth Sciences) and HPCAT at APS, which is supported by CIW, CDAC, UNLV, and LLNL through funding from DOE-NNSA, DOE-BES, and NSF. APS is supported by DOE-BES under Contract DE-AC02-06CH11357. BNL is supported by DOE under Contract DE-AC02-98CH10886. We thank Dr. Luhong Wang from HIT for helpful discussions.

■ REFERENCES

- (1) (a) Zhang, H.; Liu, C. X.; Qi, X. L.; Dai, X.; Fang, Z.; Zhang, S. C. *Nat. Phys.* **2009**, *5*, 438–442. (b) Chen, Y. L.; Analytis, J. G.; Chu, J.-H.; Liu, Z. K.; Mo, S.-K.; Qi, X. L.; Zhang, H. J.; Lu, D. H.; Dai, X.; Fang, Z.; Zhang, S. C.; Fisher, I. R.; Hussain, Z.; Shen, Z.-X. *Science* **2009**, *325*, 178–181.
- (2) Wang, G. F.; Cagin, T. *Appl. Phys. Lett.* **2006**, *89*, 152101(1–3).
- (3) (a) Nakajima, S. *J. Phys. Chem. Solid* **1963**, *24*, 479–485. (b) Anderson, T. L.; Krause, H. B. *Acta Crystallogr., Sect. B* **1974**, *30*, 1307–1310.
- (4) (a) Zhu, L.; Wang, H.; Wang, Y. C.; Lv, J.; Ma, Y. M.; Cui, Q. L.; Ma, Y. M.; Zou, G. T. *Phys. Rev. Lett.* **2011**, *106*, 145501(1–4). (b) Einaga, M.; Ohmura, A.; Nakayama, A.; Ishikawa, F.; Yamada, Y.; Nakano, S. *Phys. Rev. B* **2011**, *83*, 092102(1–4).
- (5) (a) Zhang, C.; Sun, L. L.; Chen, Z. Y.; Zhou, X. J.; Wu, Q.; Yi, W.; Guo, J.; Dong, X. L.; Zhao, Z. X. *Phys. Rev. B* **2011**, *83*, 140504(1–4). (b) Zhang, J. L.; Zhang, S. J.; Weng, H. M.; Zhang, W.; Yang, L. X.; Liu, Q. Q.; Feng, S. M.; Wang, X. C.; Yu, R. C.; Cao, L. Z.; Wang, L.; Yang, W. G.; Liu, H. Z.; Zhao, W. Y.; Zhang, S. C.; Dai, X.; Fang, Z.; Jin, C. Q. *Proc. Natl. Acad. Sci. U.S.A.* **2011**, *108*, 24–28.
- (6) (a) Sakai, N.; Kajiwara, T.; Takemura, K.; Minomura, S.; Fujii, Y. *Solid State Commun.* **1981**, *40*, 1045–1047. (b) Jacobsen, M. K.; Kumar, R. S.; Cornelius, A. L.; Sinogeiken, S. V.; Nicol, M. F. *AIP Conf. Proc.* **2007**, *955*, 171–174. (c) Khvostantsev, L. G.; Orlov, A. I.; Abrikosov, N. Kh.; Ivanova, L. D. *Phys. Status Solidi A* **1985**, *89*, 301–309. (d) Buga, S. G.; Serebryanaya, N. R.; Dubitskiy, G. A.; Semenova, E. E.; Aksenkov, V. V.; Blank, V. D. *High Press. Res.* **2011**, *31*, 86–90.
- (7) Birch, F. *Phys. Rev.* **1947**, *71*, 809–824.
- (8) Slater, J. C. *J. Chem. Phys.* **1964**, *41*, 3199–3204.
- (9) Takumi, M.; Masamitsu, T.; Nagata, K. *J. Phys.: Condens. Matter* **2002**, *14*, 10609–10613.
- (10) (a) Aoki, K.; Fujiwara, S.; Kusakabe, M. *Solid State Commun.* **1983**, *45*, 161–163. (b) Parthasarathy, G.; Holzapfel, W. B. *Phys. Rev. B* **1988**, *37*, 8499–8501. (c) Schaufelberger, P.; Merx, H.; Contre, M. *High Temp. - High Pressures* **1973**, *5*, 221–230.